Hindawi Publishing Corporation
Journal of Crystallography
Volume 2014, Article ID 862067, 9 pages
http://dx.doi.org/10.1155/2014/862067

Research Article

Crystal Structure, Spectral Studies, and Hirshfeld Surfaces Analysis of 5-Methyl-5*H*-dibenzo[*b,f*]azepine and 5-(4-Methylbenzyl)-5*H*-dibenzo[*b,f*]azepine

Madan Kumar Shankar,[1] Basavapattana C. Manjunath,[1] Koravangala Shivakumar Vinay Kumar,[2] Kudigana J. Pampa,[3] Marilinganadoddi P. Sadashiva,[2] and Neartur K. Lokanath[1]

[1] *Department of Studies in Physics, University of Mysore, Manasagangotri, Mysore 570006, India*
[2] *Department of Studies in Chemistry, University of Mysore, Manasagangotri, Mysore 570006, India*
[3] *Department of Studies in Microbiology, University of Mysore, Manasagangotri, Mysore 570006, India*

Correspondence should be addressed to Neartur K. Lokanath; lokanath@physics.uni-mysore.ac.in

Received 30 September 2013; Revised 8 December 2013; Accepted 14 February 2014; Published 19 May 2014

Academic Editor: Lígia R. Gomes

The compounds, 5-methyl-5*H*-dibenzo[*b,f*]azepine (**1**) and 5-(4-methylbenzyl)-5*H*-dibenzo[*b,f*]azepine (**2**), were synthesized and characterized by spectral studies, and finally confirmed by single crystal X-ray diffraction method. The compound **1** crystallizes in the orthorhombic crystal system in $Pca2_1$ space group, having cell parameters $a = 11.5681\ (18)$ Å, $b = 11.8958\ (18)$ Å, $c = 8.0342\ (13)$ Å, and $Z = 4$ and $V = 1105.6\ (3)$ Å^3. And the compound **2** crystallizes in the orthorhombic crystal system and space group *Pbca*, with cell parameters $a = 16.5858\ (5)$ Å, $b = 8.4947\ (2)$ Å, $c = 23.1733\ (7)$ Å, and $Z = 8$ and $V = 3264.92\ (16)$ Å^3. The azepine ring of both molecules **1** and **2** adopts boat conformation with nitrogen atom showing maximum deviations of 0.483 (2) Å and 0.5025 (10) Å, respectively. The C–H$\cdots\pi$ short contacts were observed. The dihedral angle between fused benzene rings to the azepine motif is 47.1 (2)° for compound **1** and 52.59 (6)° for compound **2**, respectively. The short contacts were analyzed and Hirshfeld surfaces computational method for both molecules revealed that the major contribution is from C$\cdots$H and H$\cdots$H intercontacts.

1. Introduction

Azepine derivatives have showed to be associated with different pharmacological activities such as antiviral, anticancer, anti-insecticidal, and vasopressin antagonist. Iminostilbene derivatives are found in montainine, coccinine, manthine, and pancracine alkaloids present in *Haemanthus* and *Rhodophiala* species [1]. They are the derivatives of drugs, such as carbamazepine [2], opipramol [3], and oxcarbazepine [4], which are used as anticonvulsants and antidepressants and in the treatment of epilepsy and trigeminal neuralgia [5]. Another compound, G32883, an iminostilbene derivative, shows effect on peripheral nerves [6]. Recently, it is reported that carbamazepine with magnesium oxide is used to treat anticonvulsant in albino rats [7]. Lateral dibenzazepine moieties are known to have potential to act as substituents for the binding site of the acetylcholine M_2 receptor [8]. The 11-phenyl-[b,e]-dibenzazepine compounds are proved to be novel antitumor compounds [9].

Synthesis and crystal structures of other iminostilbene derivatives, 5-(prop-2-yn-1-yl)-5*H*-dibenzo[*b,f*]-azepine, orthorhombic polymorph, and 5-[(4-Benzyl-1*H*-1,2,3-triazol-1-yl)methyl]-5*H*-dibenzo[b,f]azepine have been reported [10, 11]. As a part of our ongoing research on the synthesis and crystal structures and their importance of iminostilbene derivatives, we report here the synthesis and characterization by spectral studies and crystal structure using single crystal X-ray crystal diffraction of compounds 5-methyl-5*H*-dibenzo[*b,f*]azepine (**1**) and 5-(4-methylbenzyl)-5*H*-dibenzo*[b,f]*azepine (**2**). Here, we investigate the role of the main intermolecular interactions on stabilization of the

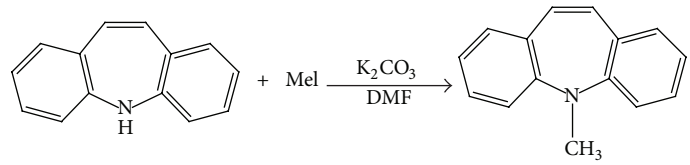

5H-Dibenzo[b,f]azepine Iodomethane 5-Methyl-5H-dibenzo[b,f]azepine

Scheme 1: The synthesis of compound **1**.

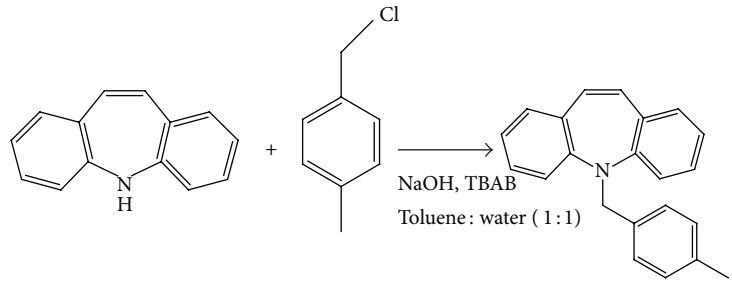

5H-Dibenzo[b,f]azepine 1-(Chloromethyl)-methylbenzene 5-(4-Methylbenzyl)-dibenzo[b,f]azepine

Scheme 2: The synthesis of compound **2.**

solid state architecture of the iminostilbene derivatives. And, Hirshfeld surface analysis and fingerprint plots analyzing intermolecular interactions were presented in the same procedure as we reported [12].

2. Material and Methods

*2.1. Synthesis of 5-Methyl-5H-dibenzo[b,f]azepine (**1**).* 5*H*-Dibenzo[*b*,*f*]azepine (0.0025 mol) was taken in dimethylformamide (DMF) solvent, and K_2CO_3 (0.0038 mol) was added at room temperature and stirred for 5 minutes. The reaction mixture was cooled to 0°C, then iodomethane was added (0.0038 mol). After 15 minutes, the resulting reaction mixture was heated at 60°C for 7 hours (Scheme 1). After completion of reaction (monitored by TLC), the reaction mixture was diluted with water (50 mL). The aqueous layer was extracted with ethyl acetate (3 ∗ 20 mL), and the combined ethyl acetate layer was washed with 0.1 N hydrochloric acid (2 ∗ 25 mL), followed by brine solution (2 ∗ 25 mL). Then, the organic layer was dried over anhydrous sodium sulfate and filtered and concentrated under reduced pressure to afford crude product, which was purified by column chromatography over silica gel (60–120 mesh) using hexane : ethyl acetate mixture in 9.5 : 0.5 ratios as eluent. The pure compound was crystallized in ethyl acetate and hexane to obtain yellow hexagonal shaped single crystals.

2.2. Spectral Data

^{1}H NMR ($CDCl_3$, 400 MHz); δ 7.21 (q, J = 4.99 Hz, 2H), 7.01–6.91 (m, 6H), 6.66 (d, J = 7.82 Hz, 2H), and 3.30 (d, J = 7.82 Hz, 2H).

Mass: Calc. 207.27 found: 208.27 (M^++1).

^{13}C NMR (100 MHz, $CDCl_3$): δ 152.28, 132.81, 132.42, 129.21, 128.90, 123.15, 118.82, and 39.30.

MS: m/z = 207.27 (calculated) m/z = 208.27 $[M+H]^+$ (found). Anal. Calcd. for $C_{22}H_{19}N_2$: C, 86.92; H, 6.32; N, 6.76.

(We also performed DEPT (distortionless enhancement by polarization transfer), which will be given as supplementary data in Supplementary Material available online at http://dx.doi.org/10.1155/2014/862067.)

*2.3. Synthesis of 5-(4-Methylbenzyl)-5H-dibenzo[b,f]azepine (**2**).* 5*H*-Dibenzo[*b*,*f*]azepine (0.0025 mol) was taken in a mixture of toluene and water in the ratio of 1 : 1, and sodium hydroxide (0.029 mol) was added followed by tetra-*n*-butylammonium bromide (TBAB) (0.00029 mol) at room temperature. After 15 minutes, 1-(chloromethyl)-4-methylbenzene (0.0031 mol) was added to the reaction mixture at room temperature. Then, the resulting reaction mixture was heated at 60°C for 5 hours (Scheme 2). After completion of reaction (monitored by TLC), the reaction mixture was diluted with water (50 mL). The aqueous layer was extracted with ethyl acetate (3 ∗ 20 mL), and the combined ethyl acetate layer was washed with 0.1 N hydrochloric acid (2 ∗ 25 mL), followed by brine solution (2 ∗ 25 mL). Then, the organic layer was dried over anhydrous sodium sulfate and filtered and concentrated under reduced pressure to afford crude product, which was purified by column chromatography over silica gel (60–120 mesh) using hexane: ethyl acetate mixture in 9.5 : 0.5 ratios as eluent. The pure

Table 1: Crystal data, data collection, and structure refinement.

Compound	**1**	**2**
Empirical formula	C15 H13 N1	C22 H19 N1
Formula weight	207.26	297.38
Temperature (K)	296	100
Wavelength (Å)	1.54178	1.54178
Crystal system	Orthorhombic	Orthorhombic
Space group	$Pca2_1$	$Pbca$
Unit cell dimension (Å)	$a = 11.5681(18)$ $b = 11.8958(18)$ $c = 8.0342(13)$	$A = 16.5858(5)$ $b = 8.4947(2)$ $c = 23.1733(7)$
Volume Å^3	1105.6(3)	3264.92(16)
Z	4	8
Calculated density g/cm^3	1.245	1.210
Absorption coefficient mm^{-1}	0.554	0.530
$F(000)$	440	1264
Crystal size mm^3	0.20 × 0.20 × 0.21	0.21 × 0.21 × 0.22
Theta range for data collection (°)	3.7 to 64.2	6.2 to 64.4
Limiting indices	$-13 \le h \le 12$ $-13 \le k \le 13$ $-6 \le l \le 9$	$-18 \le h \le 19$ $-9 \le k \le 9$ $-27 \le l \le 26$
Reflections collected/unique	9156/1417 $R(\text{int}) = 0.130$	54177/2696 $R(\text{int}) = 0.034$
Refinement method	Full-matrix least squares on F^2	Full-matrix least squares on F^2
Data/restraints/parameters	1417/1/146	2696/0/209
Goodness-of-fit on F^2	1.16	1.08
Final R indices $[I > 2\sigma(I)]$	$R_1 = 0.0786$, $wR_2 = 0.2070$	$R_1 = 0.0385$, $wR_2 = 0.0895$
Largest diff. peak and hole	−0.32 and 0.28 e Å^{-3}	−0.17 and 0.20 e Å^{-3}
CCDC	959827	958853

compound was crystallized in ethyl acetate and hexane, which yields colorless needle single crystals.

2.4. Spectral Data

^{1}H NMR ($CDCl_3$, 400 MHz); δ 7.31 (d, J = 7.56 Hz, 2H), 7.15 (T, J = 7.78 Hz, 2H), 7.05–6.99 (m, 6H), 6.92 (T, J = 7.34 Hz, 2H), 6.79 (s, 2H), 4.91 (s, 2H), and 2.16 (s, 3H).

Mass: Calc. 297.39 found: 298.39 (M^++1).

^{13}C NMR (100 MHz, $CDCl_3$): δ 150.52, 135.87, 134.51, 133.48, 131.92, 128.87, 128.70, 128.53, 128.28, 128.13, 127.50, 122.90, 120.15, 54.32, and 20.70.

MS: m/z = 297.39 (calculated) m/z = 298.39 $[M+H]^+$ (found). Anal. Calcd. for $C_{22}H_{19}N$: C, 88.85; H, 6.44; N, 4.71.

(We also performed DEPT (distortionless enhancement by polarization transfer), which will be given as supplementary data.)

2.5. Single Crystal X-Ray Diffraction Studies. X-ray intensity data were collected for **1** (hexagonal shaped) and **2** (needle shaped) using Bruker X8 Proteum diffractometer at 296 K and 100 K, respectively. Data were collected using *CuKα* radiation (λ = 1.54178 Å) with the φ and ω scan method [13]. The final unit cell parameters were based on all reflections. Data collections, integration, and scaling of the reflections were performed using the APEX2 program [13].

The structures were solved by direct methods using SHELXS [14] and all of the nonhydrogen atoms were refined anisotropically by full-matrix least-squares on F^2 using SHELXL [14]. Summary of crystal data, data collection procedures, structure determination methods, and refinement results are summarized in Table 1.

ORTEP (Figures 1 and 2) and packing diagrams (Figures 3 and 4) were generated using MERCURY [15]. And the program Crystal Explorer 3.0 [16] was used to perform Hirshfeld surfaces computational analysis and to quantify the intermolecular interactions in terms of surface contribution and generating graphical representations (Figure 5), plotting 2D fingerprint plots (Figures 6 and 8) [17], and generating

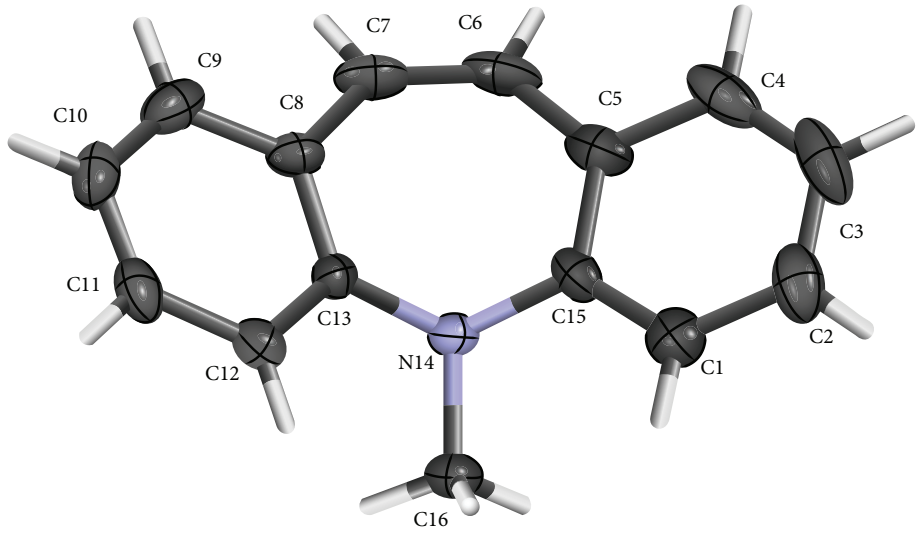

Figure 1: The molecular structure of compound **1** showing the atomic numbering system. Displacement ellipsoids are drawn at the 30% probability.

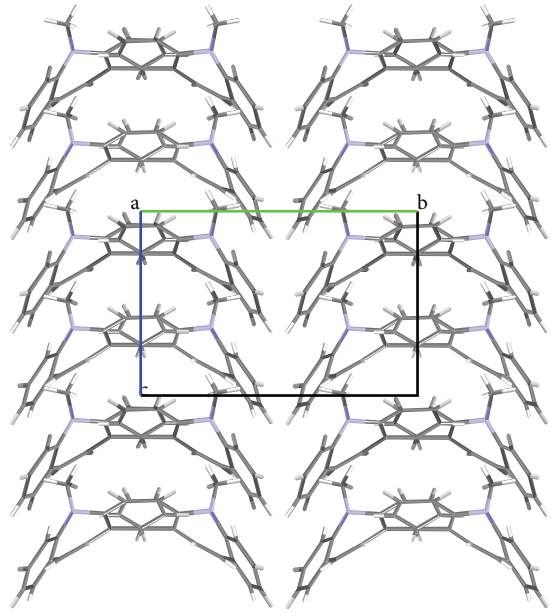

Figure 2: The crystal packing of compound **1** projected onto bc plane.

electrostatic potential (Figure 5) [18] with TONTO [19]. The electrostatic potential is mapped on Hirshfeld surfaces using Hartree-Fock (STO-3G basis set) theory over the range of −0.020 a.u. to +0.020 a.u. (Figures 5 and 7). The electrostatic potential surfaces are plotted with red region which is a negative electrostatic potential (hydrogen acceptors) and blue region which is a positive electrostatic potential (hydrogen donor).

Crystallographic data (excluding structure factors) for the structure reported in this paper have been deposited with the Cambridge Crystallographic Data Center as supplementary publications numbers 959827 (**1**) and 958853 (**2**).

3. Results and Discussion

The X-ray crystallographic analysis of **1** and **2** was performed, confirming the structures previously established by the NMR data. The crystal structure of each compound presents only one molecule in the asymmetric unit. The ORTEP diagrams of **1** and **2** including the atoms labeled are shown in Figures 1 and 3, respectively. The compounds **1** and **2** crystallize in the centrosymmetric and noncentrosymmetric space groups *Pbca* and $Pca2_1$, respectively. The structural analysis reveals that all geometric parameters agree well with the expected values reported in the literature, including the iminostilbene

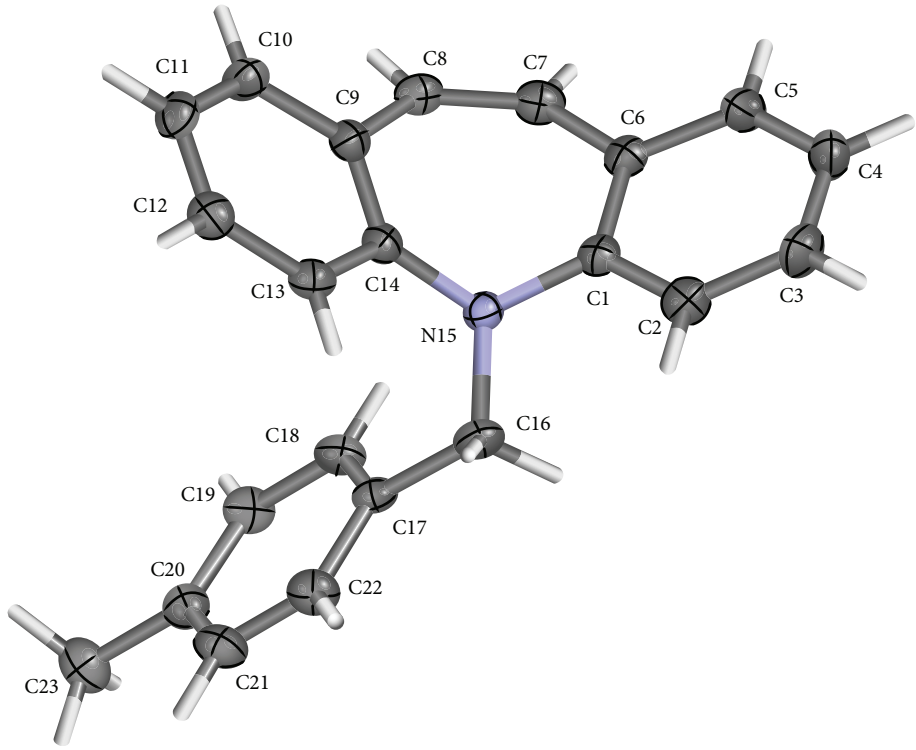

Figure 3: The molecular structure of compound **2** showing the atomic numbering system. Displacement ellipsoids are drawn at the 50% probability.

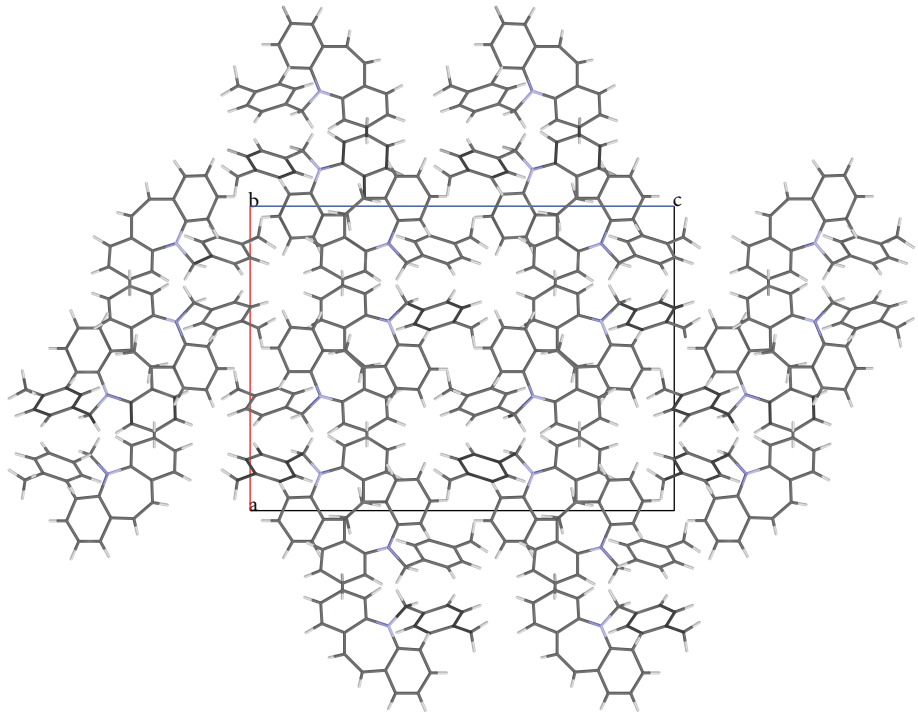

Figure 4: The crystal packing of compound **2** projected onto ac plane.

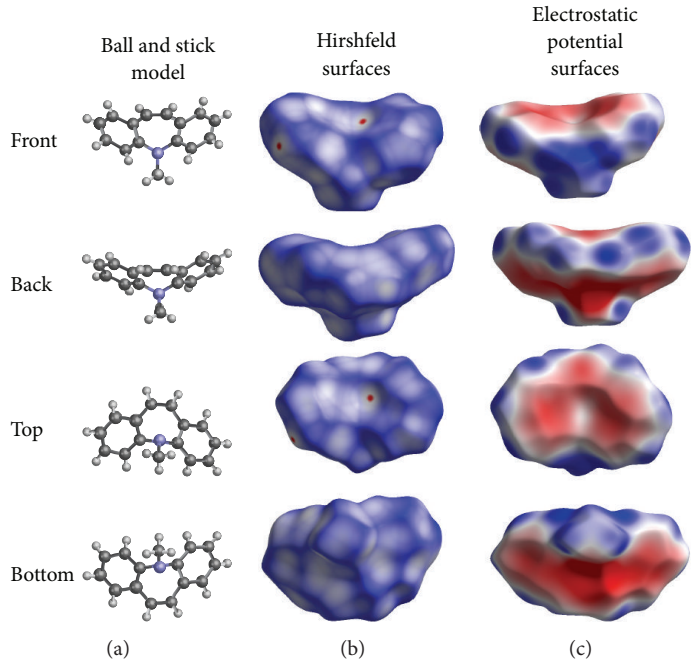

FIGURE 5: d_{norm} mapped on Hirshfeld surface (b) for visualizing the intercontacts of compound **1**. Color scale in between −0.047 au (blue) and 1.152 au (red). Electrostatic potential mapped (c) on Hirshfeld surface (different orientation) with ±0.020 au. Blue region corresponds to positive electrostatic potential and red region to negative electrostatic potential. The ball and stick model represents the different orientations (front, back, top, and bottom) and correspondingly the Hirshfeld surfaces and their electrostatic potentials are oriented.

derivatives previously published by us [10, 11]. Overall, both the molecules adopt butterfly shape and the percentage of intercontacts of **1** and **2** to the Hirshfeld surface is compared (Figure 9).

3.1. Compound 1. The fused benzene ring (C1–C5/C15 and C9–C14) to the azepine motif makes a dihedral angle of 47.1(2)°. Seven-membered (azepine) ring adopts a boat conformation with nitrogen atom showing maximum deviations of 0.483 (2) Å, the puckering parameters Q_2 = 0.663(5) Å, φ_2 = 182.1(4)°, Q_3 = 0.2050(4) Å, and φ_3 = 179.7(15)°, and the total puckering amplitude Q_T = 0.6940(4) Å [20]. The *ORTEP* of compound **1** is shown in Figure 1. The packing (Figure 2) of the molecules is stabilized with the short contacts C–H ⋯ π (Table 2), which exist between C12—H12 and the centroid (*Cg*(1): C1–C5/C15) of the ring of the neighboring molecules with a distance of 0.930 Å.

3.2. Hirshfeld Surface Analysis. Here, we estimated the intermolecular intercontacts contributing to the Hirshfeld surfaces shown in Figures 5 and 9. It shows that the major contribution is from C–H (39%) (Figures 6(d) and 9) and H–H (57%) (Figures 6(a) and 9). This is evidence that van der Waals forces exert an important influence on the stabilization of the packing in **1**. And other intercontacts C–C (2%) (Figures 6(c) and 9) and N–H (2%) (Figures 6(b) and 9) contribute less to the Hirshfeld surfaces. The mentioned intercontacts are highlighted by conventional mapping d_{norm} on the molecular Hirshfeld surfaces (Figure 5), where the red spot areas indicate intercontacts involved in the C–H ⋯ π interactions. And the electrostatic potential (Figure 7) shows the distribution of positive and negative potential over the Hirshfeld surfaces.

TABLE 2: Intermolecular interactions geometry [Å, °].

D–H⋯A	D–H (Å)	H–A (Å)	D–A (Å)	D–H⋯A(°)
1				
C12–H12⋯Cg(1)^{iii}	2.895	0.9300	3.775 (12)	166.41
2				
C3–H3⋯Cg(1)^{i}	2.990	0.7613	3.7513 (15)	141
C7–H7⋯Cg(2)^{ii}	2.880	0.8726	3.7526 (14)	156
C8–H8⋯Cg(1)^{ii}	2.620	0.8787	3.4987 (14)	159

$^{i}x-1/2, y-1/2$, and z; $^{ii}x-1, y+1/2$, and $z-1/2$; $^{iii}-x, y-2$, and $z-1/2$.

3.3. Compound 2. The fused benzene rings (C1–C6 and C9–C14) to azepine motif make a dihedral angle of 52.59(6)°. The terminal benzene ring (C17–C22) makes dihedral angles of 26.66(6)° and 77.06(6)° with benzene rings C1–C6 and C9–C14, respectively. The *ORTEP* of the compound **2** is shown in Figure 3. Seven-membered (azepine) ring adopts a boat conformation with nitrogen atom showing maximum deviations of 0.5025 (10) Å, the puckering parameters Q_2 = 0.7030(13) Å, φ_2 = 1.07(11)°, Q_3 = 0.2025(12) Å, and φ_3 = 359.2(12)°, and the total puckering amplitude

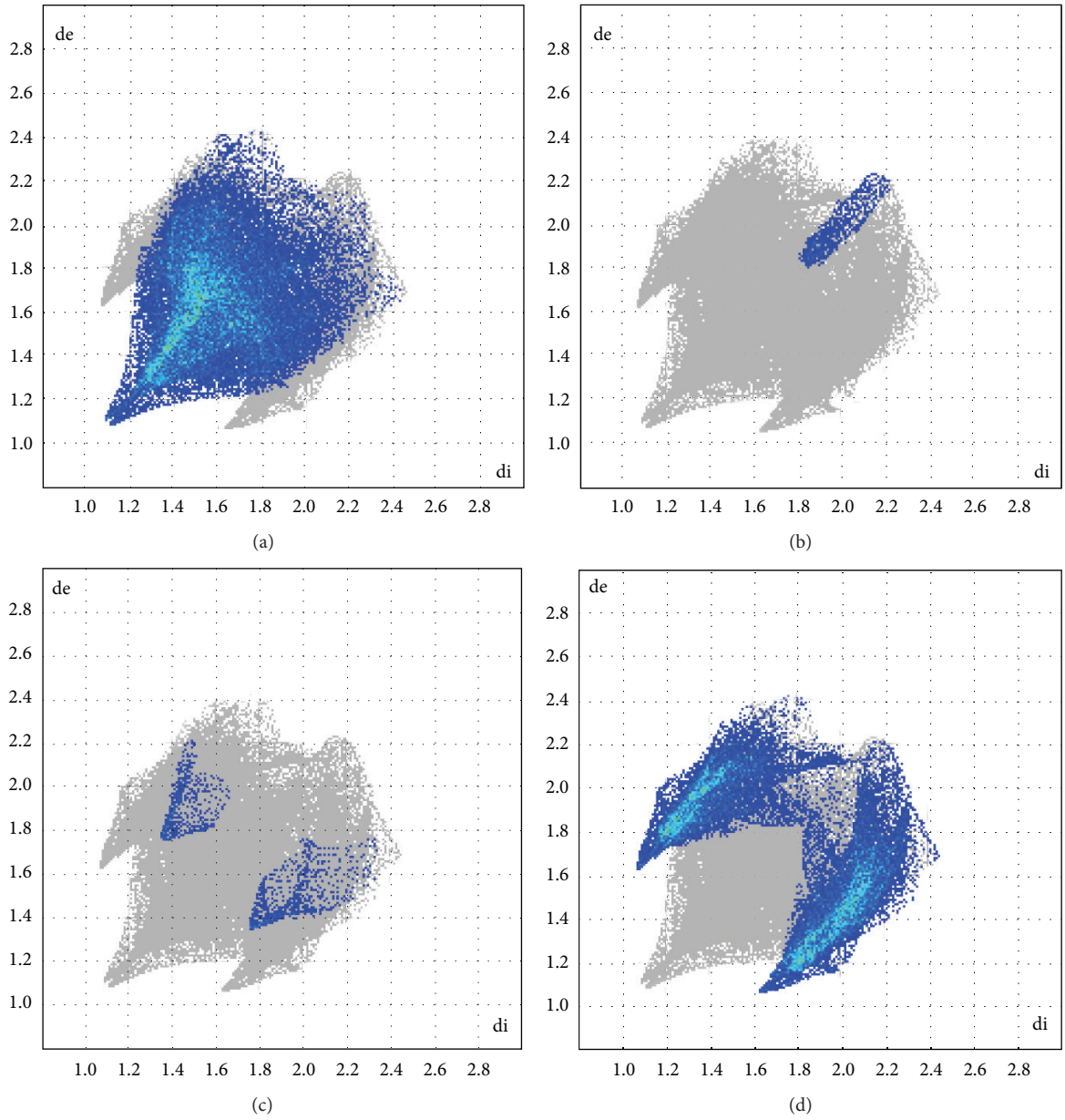

Figure 6: Fingerprint of compound **1**: (a) C···H, (b) N···H, (c) C···C, and (d) C···H. The outline of the full fingerprint is shown in gray. *di* is the closest internal distance from a given point on the Hirshfeld surface and *de* is the closest external contacts.

Q_T = 0.7315(12) Å [20]. The packing (Figure 4) of the molecules is stabilized with the short contacts of the type C–H···π (Table 2). These short contacts exist between C3–H3···*Cg*(1) with a distance 3.7513 (15) Å (angle 141°), C7–H7. . ..*Cg*(2) with a distance of 3.7526 (14) Å (angle 156°), and C8–H8···*Cg*(1) with a distance 3.4987 (14) Å (angle 159°), with *Cg*(1): C1–C6; *Cg*(2): C9–C14.

3.4. Hirshfeld Surface Analysis. The major contribution is from C—H (39%) (Figures 8(b) and 9) and H–H (61%) (Figures 8(a) and 9) intercontacts. The mentioned intercontacts are highlighted by conventional mapping d_{norm} on the molecular Hirshfeld surfaces (Figure 7). In Figure 7, the red spot areas indicate intercontacts involved in the C–H···π interactions. And the electrostatic potential (Figure 7) shows the distribution of positive and negative potential over the Hirshfeld surfaces.

4. Conclusions

Two derivatives, called 5-methyl-5*H*-dibenzo[*b*,*f*]azepine (**1**) and 5-(4-methylbenzyl)-5*H*-dibenzo[*b*,*f*]azepine (**2**), were synthesized, charactrized by spectral studies (^{1}H NMR, ^{13}C NMR and DEPT) and finally, structural elucidation by

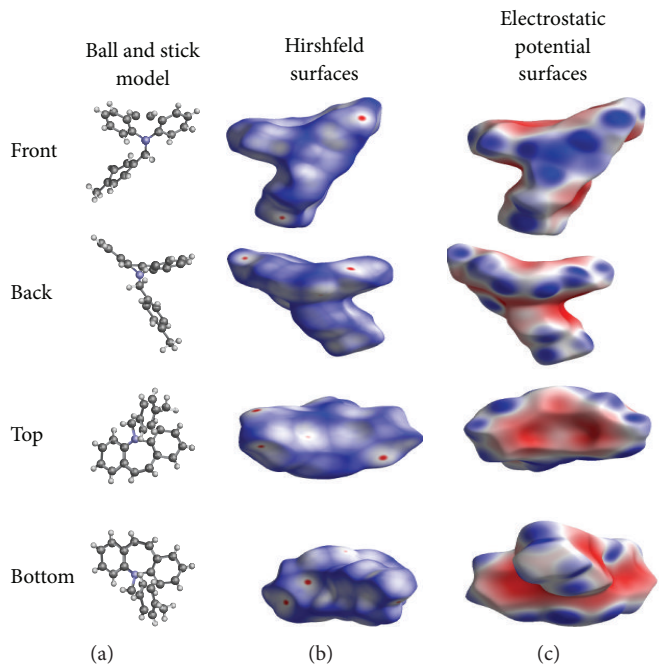

FIGURE 7: d_{norm} mapped on Hirshfeld surface (b) for visualizing the intercontacts of compound **2**. Color scale in between −0.075 au (blue) and 1.358 au (red). Electrostatic potential mapped (c) on Hirshfeld surface (different orientation) with ±0.020 au. Blue region corresponds to positive electrostatic potential and red region to negative electrostatic potential. The ball and stick model represents the different orientations (front, back, top, and bottom) and correspondingly the Hirshfeld surfaces and their electrostatic potentials are oriented.

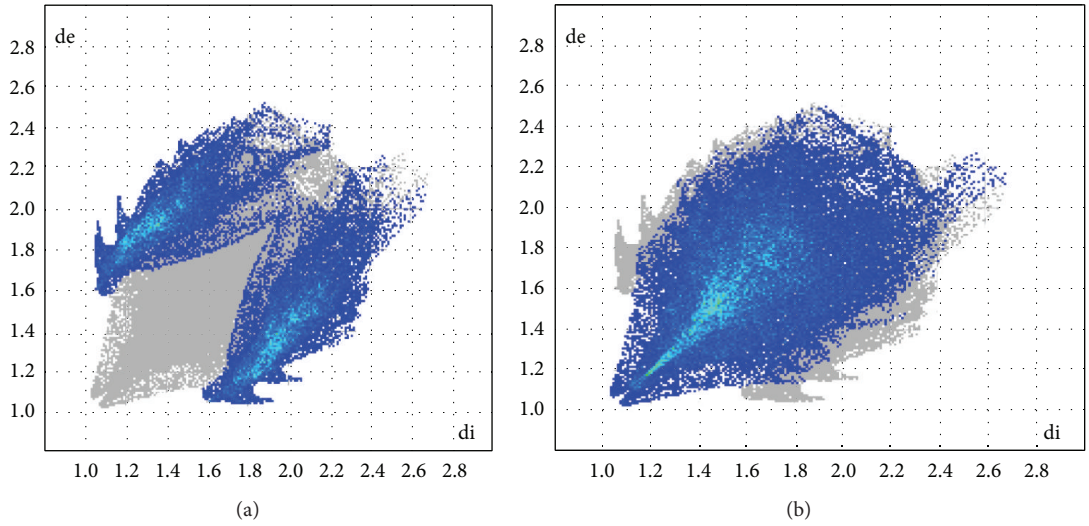

FIGURE 8: Fingerprint of compound **2**: (a) C···H and (b) H···H. The outline of the full fingerprint is shown in gray. *di* is the closest internal distance from a given point on the Hirshfeld surface and *de* is the closest external contacts.

single crystal X-ray diffraction studies. The azepine rings of compounds **1** and **2** adopt the boat conformation, and, as a whole, molecule assumes butterfly shape. The fused benzene ring to azepine motif makes a dihedral angle of 47.1 (2)° for compound **1** and 52.59 (6)° for compound **2**, respectively. Hirshfeld surface analysis of **1** and **2** reveals that H···H and C···H are the most abundant intercontacts. This is evidence that van der Waals forces exert an important influence on the stabilization of the packing in **1** and **2**.

Conflict of Interests

The authors declare that there is no conflict of interests regarding the publication of this paper.

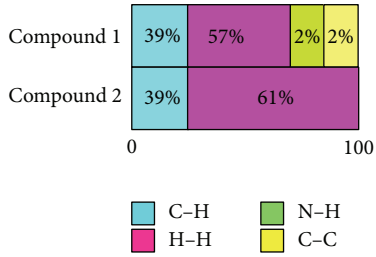

Figure 9: Hirshfeld surfaces percentage evaluation of short contacts for compound **1** and compound 2. The particular squared colour boxes on the right side represent the type of the intercontact visible at the percentage evaluation boxes.

Acknowledgment

The authors thank Institution of Excellence, University of Mysore, Mysore, for providing single crystal X-ray diffractometer and NMR facility for data collection.

References

[1] P. Panneerselvam, K. Sandya, and K. Vijayalakshmi, "Dibenazoazepine, a pharmacologically active moiety," *ISOR Journal of Applied Chemistry*, vol. 1, no. 6, pp. 41–44, 2012.

[2] B. W. Rockliff and E. H. Davis, "Controlled sequential trials of carbamazepine in trigeminal neuralgia," *Archives of Neurology*, vol. 15, no. 2, pp. 129–136, 1966.

[3] H.-J. Möller, H.-P. Volz, I. W. Reimann, and K.-D. Stoll, "Opipramol for the treatment of generalized anxiety disorder: a placebo-controlled trial including an alprazolam-treated group," *Journal of Clinical Psychopharmacology*, vol. 21, no. 1, pp. 59–65, 2001.

[4] P. C. Fuenfschilling, W. Zaugg, U. Beutler et al., "A new industrial process for oxcarbazepine," *Organic Process Research and Development*, vol. 9, no. 3, pp. 272–277, 2005.

[5] M. P. Sadashiva, B. H. Doreswamy, Basappa, K. S. Rangappa, M. A. Sridhar, and J. S. Prasad, "Synthesis and crystal structure of 5-allyl-5*H*-dibenzo[*b,f*]azepine," *Journal of Chemical Crystallography*, vol. 35, no. 3, pp. 171–175, 2005.

[6] H. Honda and M. B. Allen, "The effect of an iminostilbene derivative (G32883) on peripheral nerves," *Journal of the Medical Association of Georgia*, vol. 62, no. 2, pp. 38–42, 1973.

[7] N. A. Patil, H. S. Somashekar, S. Narendranath, P. Prashanth, S. K. Reddy, and A. Bhandarkar, "Evaluation of anticonvulsant activity of magnesium oxide alone and along with carbamazepine," *Asian Journal of Pharmaceutical and Clinical Research*, vol. 5, no. 2, pp. 142–145, 2012.

[8] R. Li, C. Trankle, K. Mohr, and U. Holzgrabe, "Hexamethonium-type allosteric modulators of the muscarinic receptors bearing lateral dibenzazepine moieties," *Archiv der Pharmazie*, vol. 334, no. 4, pp. 121–124, 2001.

[9] R. A. Al-Qawasmeh, Y. Lee, M.-Y. Cao et al., "11-phenyl-[b,e]-dibenzazepine compounds: novel antitumor agents," *Bioorganic and Medicinal Chemistry Letters*, vol. 19, no. 1, pp. 104–107, 2009.

[10] M. M. M. Abdoh, S. Madan Kumar, K. S. Vinay kumar, B. C. Manjunath, M. P. Sadashiva, and N. K. Lokanath, "5-(prop-2-yn-1-yl)-5*H*-dibenzo[*b,f*]-azepine: orthorhombic polymorph," *Acta Crystallographica E*, vol. 69, p. o17, 2013.

[11] B. C. Manjunath, K. S. Vinay Kumar, S. Madan Kumar, M. P. Sadashiva, and N. K. Lokanath, "5-[(4-benzyl-1*H* -1,2,3-triazol-1-yl)methyl]-5*H* -dibenzo[*b,f*]azepine," *Acta Crystallographica E*, vol. 69, p. o1233, 2013.

[12] S. Madan Kumar, B. C. Manjunath, G. S. Lingaraju, M. M. M. Abdoh, M. P. Sadashiva, and N. K. Lokanath, "A Hirshfeld surface analysis and crystal structure of 2′-[1-(2-fluoro-phenyl)-1*H*-tetrazol-5-yl]-4-methoxy-biphenyl-2-carbaldehyde," *Crystal Structure Theory and Applications*, vol. 3, pp. 124–131, 2013.

[13] Apex2 (Version 2013), *Program for Bruker CCD X-Ray Diffractometer Control*, Bruker AXS Inc., Madison, Wis, USA, 2013.

[14] G. M. Sheldrick, "A short history of SHELX," *Acta Crystallographica A*, vol. 64, no. 1, pp. 112–122, 2008.

[15] C. F. Macrae, I. J. Bruno, J. A. Chisholm et al., "*Mercury CSD 2.0*—new features for the visualization and investigation of crystal structures," *Journal of Applied Crystallography*, vol. 41, no. 2, pp. 466–470, 2008.

[16] S. K. Wolff, D. J. Grimwood, J. J. McKinnon, D. Jayatilaka, and M. A. Spackman, *CrystalExplorer 3.0*, University of Western Australia, Perth, Australia, 2001.

[17] M. A. Spackman and J. J. McKinnon, "Fingerprinting intermolecular interactions in molecular crystals," *CrystEngComm*, vol. 4, no. 66, pp. 378–392, 2002.

[18] M. A. Spackman, J. J. McKinnon, and D. Jayatilaka, "Electrostatic potentials mapped on Hirshfeld surfaces provide direct insight into intermolecular interactions in crystals," *CrystEngComm*, vol. 10, no. 4, pp. 377–388, 2008.

[19] D. Jayatilaka, D. J. Grimwood, A. Lee et al., *TONTO—A System for Computational Chemistry*, The University of Western Australia, Nedlands, Australia, 2005.

[20] D. Cremer and J. A. Pople, "A general definition of ring puckering coordinates," *Journal of the American Chemical Society*, vol. 97, no. 6, pp. 1354–1358, 1975.